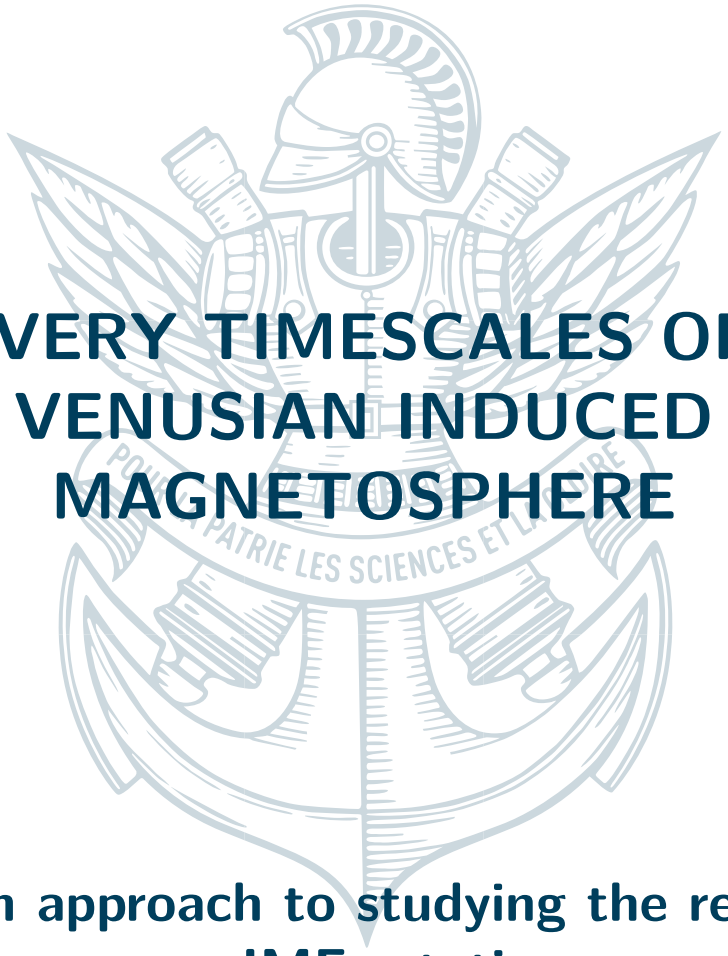

RECOVERY TIMESCALES OF THE VENUSIAN INDUCED MAGNETOSPHERE

Simulation approach to studying the response to an IMF rotation

Final written report: August 15th, 2024

Ben Ghali Khalil X2021

ÉCOLE POLYTECHNIQUE

INSTITUT POLYTECHNIQUE DE PARIS

IRF INSTITUTET FÖR RYMDFYSIK
Swedish Institute of Space Physics

ACKNOWLEDGMENTS

First of all, I would like to offer my utmost gratitude to the whole team of the IRF Uppsala for their warm welcome and hospitality both within and outside of the work environment. I felt truly welcome as a member of this highly competent team and was glad to interact with them daily either casually or by participating in the various team meetings that offer a wide view on the field of research in space physics and the works of each member.

This internship has thus allowed me to have a peek on the works of many experts in this fields as well as the different aspects of being a contributor to space physics at different levels and positions.

I was also able to forge very strong bonds within the context of this work and am glad to have met many people that I am now able to call friends. I hope that in the future I will also be able to keep in touch with everyone and maybe even collaborate with some on future projects.

It goes without saying that I am very thankful to both my supervisors, *Moa PERSSON* and *Sae AIZAWA*, for their continuous guidance and reassurance and for taking the time to allow me this opportunity of working under them on this project. I couldn't have wished for any better supervisors and I hope that I was able to match their expectations and offer something of value to them in return.

They both have taught me so much not only about the subject at hand, but also more broadly about life as a researcher and the joys and struggles of research in space physics. I feel much more in touch with this community than I was a few months ago and look forward to becoming a more active part of it in the future.

Finally, I am ever as grateful to Ecole Polytechnique and my professors, in particular to *Fouad SAHRAOUI*, for offering me this precious opportunity and allowing me to have this immersive experience within the field of research in a highly skilled team and an exemplary work environment.

TABLE DES MATIÈRES

1 ABSTRACT

Venus creates an induced magnetosphere from its interaction with the solar wind, consisting of different regions by various plasma boundaries. The characteristics of this induced magnetosphere are highly dependant on the solar wind and *Interplanetary Magnetic Field (IMF)* properties and its orientation in particular is influenced by variations in the IMF.
Investigations of the effect that the IMF variations have on the Venusian Induced Magnetosphere can help us understand the interactions of Venus and other unmagnetized planets with their surrounding.

Historically, Venus has been the target of study of space exploration missions such as the most recent *Venus Express (VEX)* (2005-2014) or the preceding *Pioneer Venus Orbiter (PVO)* (1978-1992). It has also been a popular spot for fly-bys for many space missions. But despite the vast amount of data from measurements that have been collected in the Venusian vicinity, the events that we are interested in require multiple spacecrafts to combine multi-space measurements. This is why simulations come in as a strong tool to study these interactions.

In this study, we take this simulation-based approach to determine the recovery timescales of the Venusian induced magnetosphere in response to IMF rotation. Based on a time-dependent *(Latmos Hybrid Simulation, LatHyS)* and in-situ measurements from a *BepiColombo* fly-by (August 10, 2021) for setting the solar wind conditions and the IMF parameters, we determine the profile of the magnetospheric response in different areas of the Venusian nightside due to IMF rotations.

2 INTRODUCTION

Venus is the second closest planet to the sun in the solar system, preceded by Mercury and followed by Earth. Venus is sometimes called Earth's "sister planet" as they are very similar in terms of mass and diameter and is therefore an interesting planet to study to learn more about our home planet and . Nevertheless, Venus differs radically from earth in more than one way.

First of all, the planet's atmosphere is much thicker and CO_2 heavy than that of earth. In fact, the atmospheric pressure on its surface is about 92 times greater than Earth's, and the atmosphere is composed of around 96% carbon dioxide, 3% nitrogen and 1% other gases. Its Ionosphere is formed by the interaction between particles of the atmosphere with the energetic solar ultraviolet flux that ionizes these particles.

Venus has no intrinsic magnetic field, however an induced magnetosphere is created as the ionized top layer of its thick atmosphere directly interacts with the solar wind and the *interplanetary magnetic field (IMF)*[4]. The characteristics of the Venusian induced magnetosphere are the direct consequence of and therefore ordered by the structure of the upstream solar wind and IMF. Variations in the IMF and the solar wind will thus create variations in the induced magnetosphere, which have consequences for the atmospheric escape and subsequently the Venusian atmospheric evolution.

The planet also interacts with the Solar Wind in a similar way to Earth, deviating and accelerating the flow of the plasma around the planet and guiding it downstream creating some well known draping shape for the magnetic field lines around the planet which are carried by these plasma particles. Similar plasma boundaries and areas to those observed around earth's vicinity are observed in the induced magnetosphere of Venus.

Given the wide range of processes acting on the magnetosphere, it is challenging to quantify the degree to which changes in each of the external and internal conditions might affect the overall interaction. Furthermore, exactly how a rotation of the IMF affects the induced magnetotail and the ion escape is not yet fully explored. Despite having been the subject of in-depth studies by several spacecrafts in the history of space exploration, such transient events are not simple to measure with a single orbiting spacecraft. Instead we can rely on results from models which is the approach we took for this project.

Specifically, we rely on a *global hybrid simulation* model which was adapted to Venus *(Latmos Hybrid Simulation, LatHyS)*. This model allows for a time varying rotation of the IMF inside one simulation, which gives an opportunity to observe the reaction of the Venusian induced magnetosphere in real time. We may also investigate how quickly the induced magnetosphere adapts to the rotation. These simulations also allow us to isolate parameters such as the rotation speed and angle and thus study the effect each has on the magnetospheric recovery timescales. In this study, we analyze runs of these simulations with different speeds for an IMF rotation of 90 degrees. The rotations happen while maintaining the upstream solar wind conditions such as density and velocity. The rotations, during which the IMF amplitude is kept constant, last for 42s, 83s or 167s depending on the case.

This study is structured as follows : The methodology for our simulation runs as well as the data analysis are explored in a first section. The following section is dedicated to the results of our study and their interpretation. Finally, a section is dedicated to conclusions and discussions as well as future perspectives and unanswered questions.

3 METHODOLOGY

3.1 LatHys Simulations

Latmos Hybrid Simulation (LatHyS) is a hybrid simulation model for Mars-Solar wind interaction which was adapted to Venus (among other astral bodies). It is derived from a first version described in *Modolo et al. (2016)*[7]. The hybrid trait of the model means that it treats the ions kinetically by solving the Lorentz equation of motion, while electrons are treated as a mass-less charge-neutralizing fluid.

The use of hybrid models in opposition to simpler *MagnetoHydroDynamic (MHD)* models is important to properly understand the interaction between the solar wind plasma and the Venusian environment at the ion kinetic scale. Although MHD models are able to reproduce some of the global characteristics of the solar wind interaction with Venus, they do not take into account the particle behavior.
Neutral species and planetary ions are implemented in hybrid models, but most of them rely on the use of simplified neutral atmospheres and exospheres, with no internal dynamics, and simplified ion production descriptions. Despite these limitations, the ion escape rates estimated by these models match very well with observations[2].

3.2 Hybrid formalism

Hybrid models are an intermediate approach, between three-dimensional fully kinetic models and ideal MHD models. They consist of representing the electrons as a fluid playing mainly a plasma charge neutralizing role, while ions are modeled by individual cells representing clouds of ions with the same properties (ions with the same charge, mass, velocity). These macroparticles are characterized by the density of ions within.

The position and velocity of these macro-particles obey to laws of motion of physical particles under the action of the Lorentz forces ($m\frac{d^2r}{dt} = q(E + v \times B)$).

For the massless electron fluid, the alternative to the momentum equation takes the form of the standard generalized Ohm's law.

The magnetic and electric fields are obtained by solving Maxwell's equations.

3.2.1 • The Venusian environment

The simulation is described in the Venus-Solar-Orbital (VSO) coordinates system.
— X is taken along the Sun-Venus direction, positive towards the Sun
— Z is colinear to the Venus orbital angular momentum around the sun
— Y completing the right hand coordinate system

Distances are all normalized and expressed in planetary radii [$R_v = 6052km$].
An open boundary is used in the X-direction while a periodic boundary is used in both the Y- and Z-directions.

The numerical scheme used in LatHyS for Venus is the same as the one used for the other planetary environments. The solar wind consists of two ion species while the Venusian environment consists of various neutral particle and derived ion species which are present in different layers of the planetary environment. The H, O, and CO_2 particles populate the Exosphere, while the Ionosphere is derived from the ionization of these particles via chemical reaction embedded in the model. It consists of H^+, O^+, O_2^+ and CO_2^+ ions. The study of the recovery timescales of the O^+ plume is also of interest to us during this study. Studies show that recovery time ranges within the order of the magnetosheath O^+ gyroperiod[10], showing the kinetic nature of the plume recovery process.

3.2.2 • Parameters

The choice of physical parameters is crucial to make sense of the simulation's outcome and results. In this study, a realistic model is calibrated with parameters from in-situ measurements of an IMF rotation event that was captured by BepiColombo during its 2nd Venus flyby in August 10, 2021. In this study, we will use the same parameters as Aizawa et al. (2022) who studied the response of the venusian environment during this event to further understand and interpret the data at hand through the same hybrid simulations, anchoring them as a powerful and necessary tool for the understanding and expanding on the inevitably limited measurements that spacecrafts provide.

Among the parameters that we can tweak for each simulation, some are specific to the planetary environment and the solar wind characteristics such as its density, velocity and the IMF orientation, and others are more event-related and dictate the angle of the IMF rotation and the time frame during which it occurs. Each routine also can be run with a specific grid size and resolution as well as a pre-defined time step chosen carefully to ensure a compromise between accurate results and a realistic runtime. This is why the parallelization in the computations for the spacial evolution at each time-step between the cores of the server-provided CPU is necessary to guarantee efficiency and allow running thorough simulations in a reasonable time-frame. The memory cost of each simulation, highly correlated with the spacial resolution and size of the grid, has to be taken into account as its cost may exceed the limited resources offered by the server.

Time resolution The time-dependent simulation is expressed in normalized time-steps according to the ion cyclotron or gyrofrequency. In our specific runs, this gyrofrequency equates to $7.182.10^{-1}$ $rad.s^{-1}$.
The normalized time unit is equal to the inverse of this frequency or specifically 1.3924 s.

For our simulations, we chose to run with time steps of 0.03 normalized time units or $1.3924 * 0.03 \approx 0.042$ s. It is important for the time steps to be negligible in comparison to ion specific timescales such as the gyrofrequency in order for the step-by-step linear approximation of the motion differential equations for the ions to be valid and yield realistic results.

Spacial resolution The time-dependent simulations analyzed in this work have a 178 km spacial resolution, or about 0.03 planetary radii ($R_V = 6052km$).
The grid shape extends from the center of the planet $(0, 0, 0)$ to $+2.0$ R_V and -4.0 R_V in the X direction. Whereas the YZ boundaries are around $+5.0$ R_V and -5.0 R_V.
It is important to have such extended boundaries in the Y and Z directions to avoid "unwanted" interactions due to the connected boundaries in both these directions. In fact no boundary conditions are set and the edges are instead connected in a circular way for both the Y and Z coordinates.

Solar wind characteristics For the solar wind specific arguments, values were chosen according to the above mentioned BepiColombo observations for the basic run. This yielded a density of 14.7 cm^{-3} and a velocity of 338 $km.s^{-1}$. These parameters were our starting point for our test runs but were not restrictive, as taking interest in the effect of variations within these parameters naturally led to running similar simulations while isolating the effect of each parameter by varying it and maintaining the others in order to compare the results with test simulations.
The BepiColombo observations also provided values for the IMF amplitude and orientation, especially the angle that the IMF makes with the YZ-plane, also referred to as the *Parker Angle*. In fact, this phenomenon is due to the ballerina's skirt shape or *Parker Spiral* of the heliospheric current sheet that leads to wider angles for further planets from the sun.
The upstream IMF amplitude and Parker angle are maintained through the routine as the YZ-plane rotation (around the X-Axis) or **clock angle** rotation of the IMF is applied. Solar wind velocity is also unchanged during this routine.

Rotation parameters Throughout this study, 90 degree rotations are applied to the IMF during different time periods in order to study the recovery of the Venusian Induced Magnetosphere. Comparison between relatively faster and relatively slower rotations are made in this paper.

3.3 Data classification

The natural step following the simulation runs is the analysis of the results offered by said simulations. In order to do so, the data obtained needs to first go through some post-treatment to combine the results into specific and easy to understand formats, paving the way for easier data analysis and classification.
Moreover, the Venusian environment and in particular its induced magnetosphere being shaped into different areas that behave differently in terms of dominant forces or ion composition, it is only natural that different areas show different responses to the IMF rotation. Hence a big part of the analysis work is identifying and seperating each area in an attempt to study its specific response and recovery timescale.

In the following section, we define the methods used to define different areas and to study each area and the phenomenon that lead to the delay in the rotation recovery. We start by exploring the Venusian Environment in an effort to define the different areas of interest to have a more precise study of the recovery timescales for each area.

3.3.1 • Boundaries

The aim of this section is to describe the methods used to define and to determine the boundaries that seperate the areas of study. This requires a thorough exploration of the Venusian Environment and its induced magnetosphere in particular.
Decades of studies and in-situ measurements have led us to a relatively precise understanding of Venus' induced magnetosphere among other unmagnetized planets like Mars[5] and the different areas composing their Magnetosheathes.

Venusian environment : Despite the absence of an intrinsic magnetic field, the interaction of the solar wind with Venus gives a similar result to its interaction with magnetized planets.

For starters, we notice the formation of a **Bow Shock (BS)** as the supersonic and super-Alfvénic solar wind meets the conductive ionosphere, seperating the solar wind environment from the Venusian Magnetosheath.
The BS is the result of accumulation of shocked solar wind plasma that is slowed, heated, and deflected. It can be determined as the area where pressure equality $P_{dyn} = P_{th}$ between plasma dynamic pressures and thermal pressures is attained.
Models have long been used as an accurate approximation of the Bow Shock's shape. Conic curve models in particular have been fitted through observation and measurements to describe the Venusian Bow Shock to a somewhat accurate degree, despite not taking into account asymmetries and the influence of the solar cycle or upstream conditions such as the solar wind dynamic pressure that affect the Bow Shock location[11].

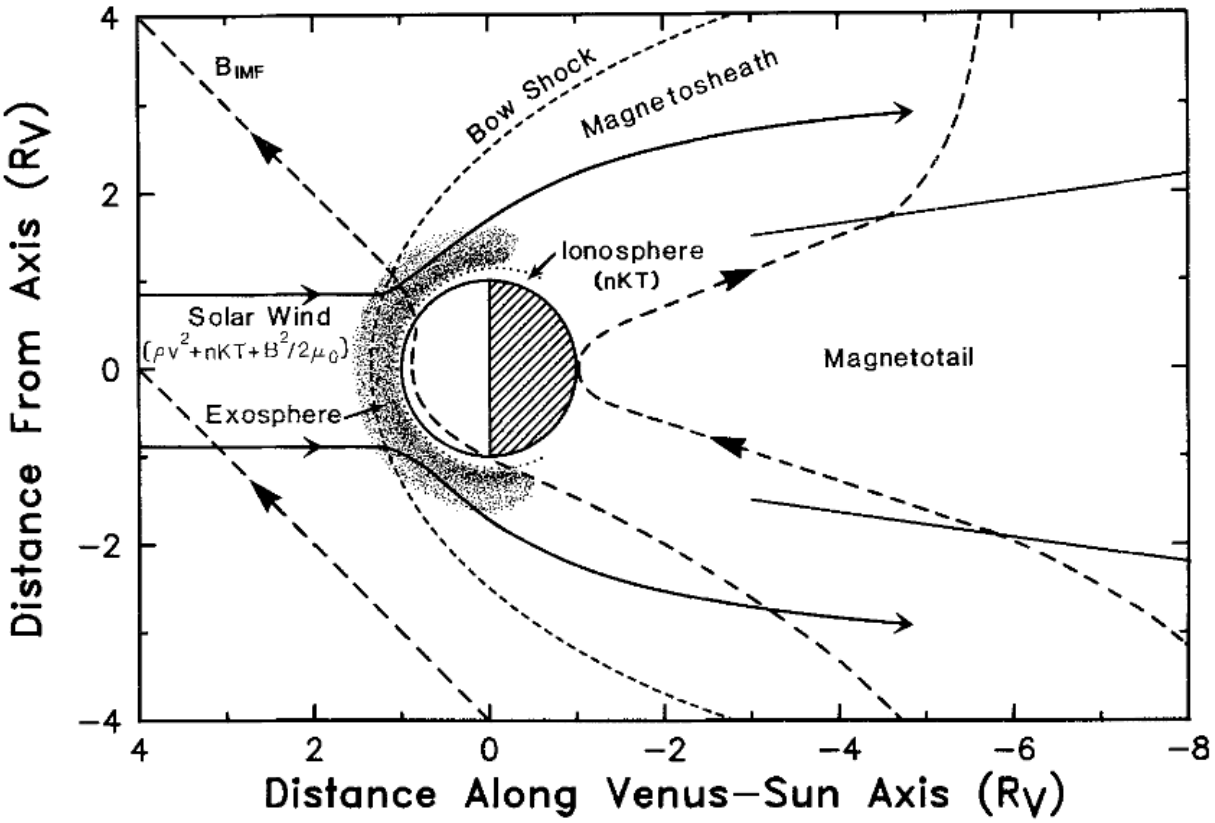

FIGURE 1 – The Magnetosheath and Magnetotail of Venus **(Philips et al. (1991))**[9]

Many other transitions within the BS area can be of interest to us and depending on which parameters are examined or which plasma processes are in focus, we may identify several different boundaries.

In the following study, we consider the **Magnetic Pile-up Boundary (MPB)** as a barrier of interest separating the ionospheric plasma from the shocked, magnetized plasma in the magnetosheath[6].
Within this area, a larger time shift and a smoother rotation of the local magnetic field is expected due to the relatively smaller bulk velocity of the local plasma in this region, the energy exchange across the MPB, and the magnetic field diffusion into the Venusian ionosphere.
The Magnetic Pile-up region can be determined as the area where the magnetic pressure $P_{mag} = \frac{B^2}{2\mu_0}$ dominates over the plasma ion thermal pressure $P_{th} = nk_BT$.
Within this region, we can observe a decrease in suprathermal electron energy fluxes and magnetic field fluctuations.

The MPB can then be determined as the area where pressure equality $P_{th} = P_{mag}$ between plasma thermal pressure and magnetic pressure is attained.

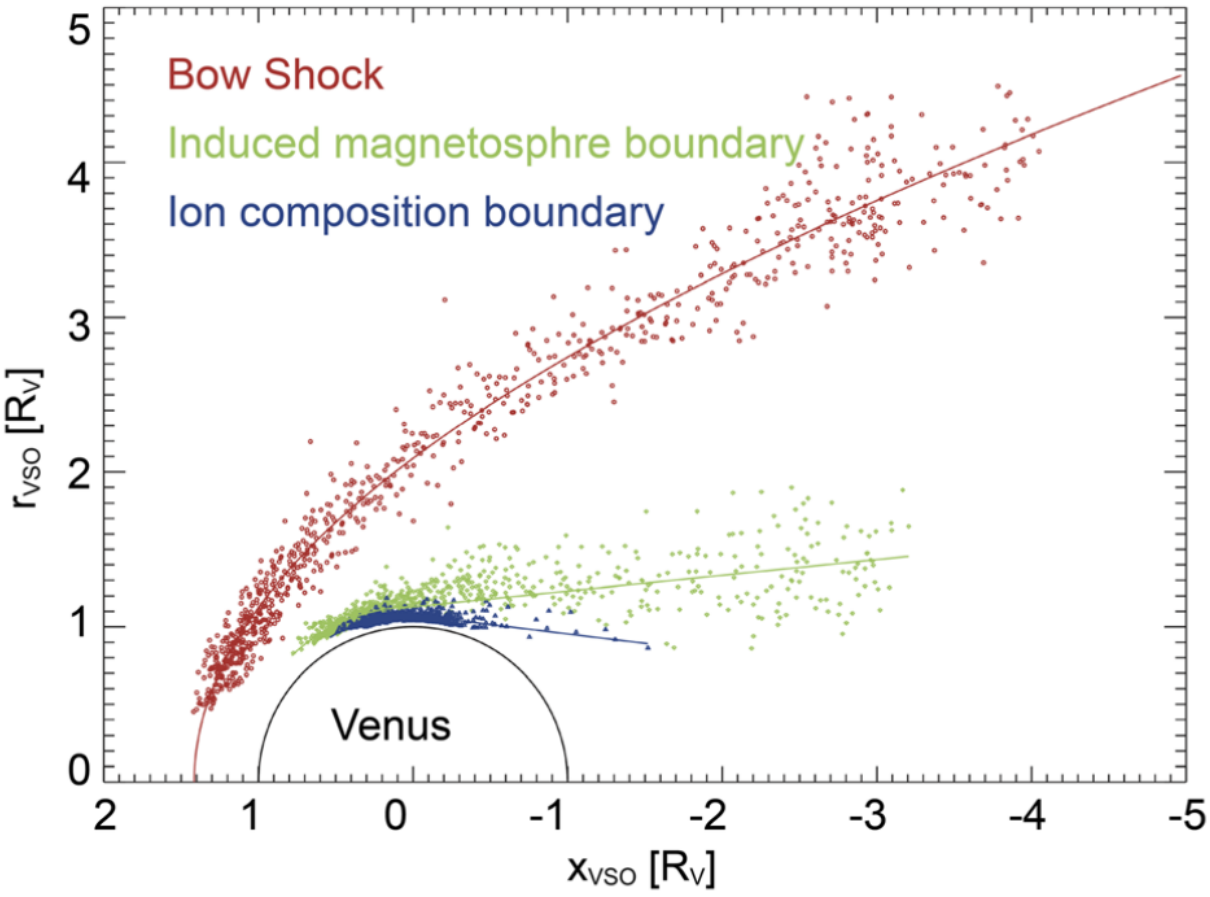

FIGURE 2 – VEX measurements of the positions of three different plasma boundaries shown in a cylindrical coordinate system **(Fuutana et al. (2017))**[1]

Boundary derivation : Plasma pressure balance is an important criterion for determining the boundaries previously defined and will be crucial in defining areas of interest for our study. The plasma pressure terms are estimated using the following equations :

— The solar wind dynamic pressure P_{dyn} is estimated from both ion density n and speed U simulation local values, and proton mass m_p using

$$P_{dyn} = m_p n U^2$$

— The total magnetic pressure P_{mag} is calculated from the local magnetic field value B and the vacuum permeability μ_0 as

$$P_{mag} = \frac{B^2}{2\mu_0}$$

— The thermal pressure P_{th} of the magnetosheath is estimated from the ion density and temperature and is obtained through

$$P_{th} = n k_B T$$

The MPB is therefore approximated locally for each plane cut orthogonal to the X axis.

Pressure values are averaged for cylindrical radius within each plane in order to calculate an average pressure difference per distance from the center.
We then approximate the MPB from the pressure balance as a circular symmetric boundary with radius that equalizes the average plasma thermal pressure and magnetic pressure.

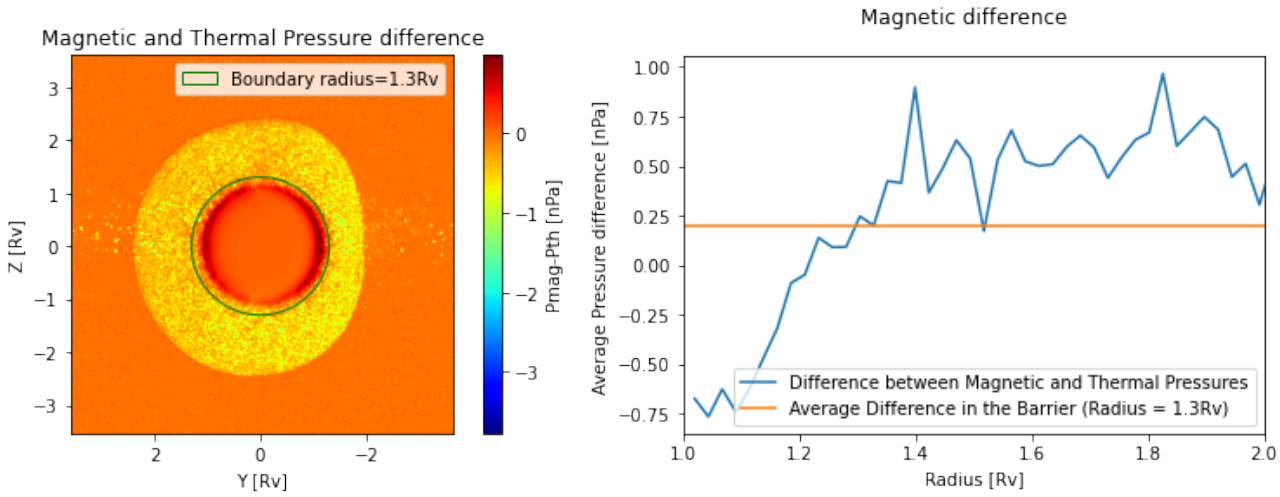

FIGURE 3 – Determination of the MPB in the terminator

Figure 3 shows a cut of the difference between Magnetic and Thermal pressures in the terminator plane. The left figure shows the overall profile of this difference in space, whereas the second plots the average value of pressure differences according to the distance from the center along a cut in the Terminator plane. This simplification in cylindrical symmetry nevertheless can be used as a good criterion for finding circular boundaries that approach the actual physical boundaries.

For simplicity's sake, the BS is determined from a fitting of a cylindrically-symmetric conic curve[3] defined by the following equation in the polar coordinates :

$$r = \frac{L}{1 + \epsilon \cos(\theta)}$$

where $r = \sqrt{(x - x_0)^2 + y^2 + z^2}$ and $\theta = \arccos \frac{x - x_0}{r}$

The fitting coefficients obtained from least square fitting with measurements from observed bow shock crossings are the following[3] :

— The eccentricity of the conic curve $\epsilon = 1.028 \pm 0.010$
— The focus point $x_0 = (0.691 \pm 0.032) R_V$
— The semilatus rectum $L = (1.499 \pm 0.041) R_V$

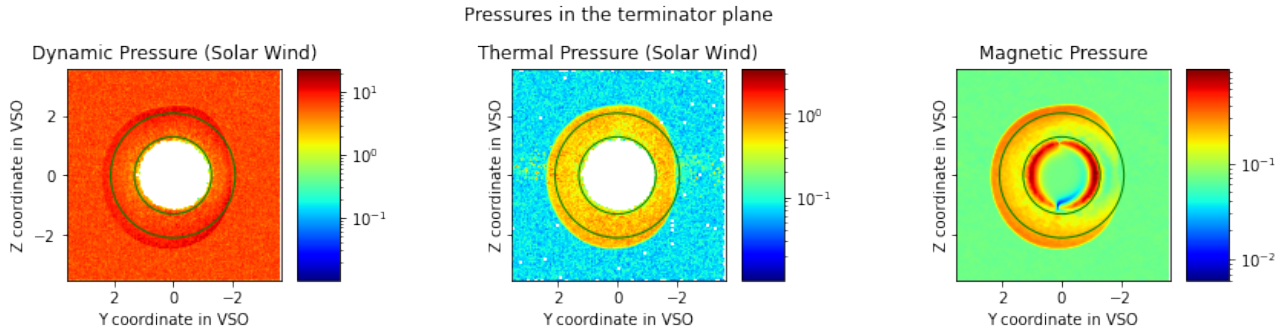

FIGURE 4 – Pressure values in the terminator : Green circles represent the estimated BS and MPB that have consecutive radii of $2.1R_V$ and $1.3R_V$

3.3.2 • AREA DEFINITION

As we will show further in this study, the time delays for the adaptive rotation of the Venusian induced magnetosphere in response to the IMF rotation can be linked to the material propagation times for the solar wind ions carrying the rotations at hand.
An expected outcome is therefore that time delays are all the greater the further downstream and the more inward or closer to the planet, where the plasma is slowed down and more deflected.
Therefore, to take into account the time delay that is associated with :

- The magnetic perturbation propagation downstream
- the convection of the perturbation through the magnetosphere

We study different timescales for seperate regions :

- With different positions in the Sun-Venus direction
- According to the position within the magnetosphere

For the analysis of the rotation response, the study is then divided into different planes normal to the X axis, which is the axis of the solar wind propagation in the simulations.
Within each plane, annular areas are seperated by the previously defined boundaries in an effort to study each area seperately.

Planes Focusing on the study of the downstream response to the IMF rotation, we decided to settle on three planes equally distant from each other and each at different distances from the planet center

- The first plane will be the **terminator** that slices through the planet center at $X = 0.0R_V$
- Then parallel equidistant planes at respectively $X = -1.3R_V$ and $X = -2.6R_V$ are studied as representatives of the magnetosheath both closer to the planet and further downstream

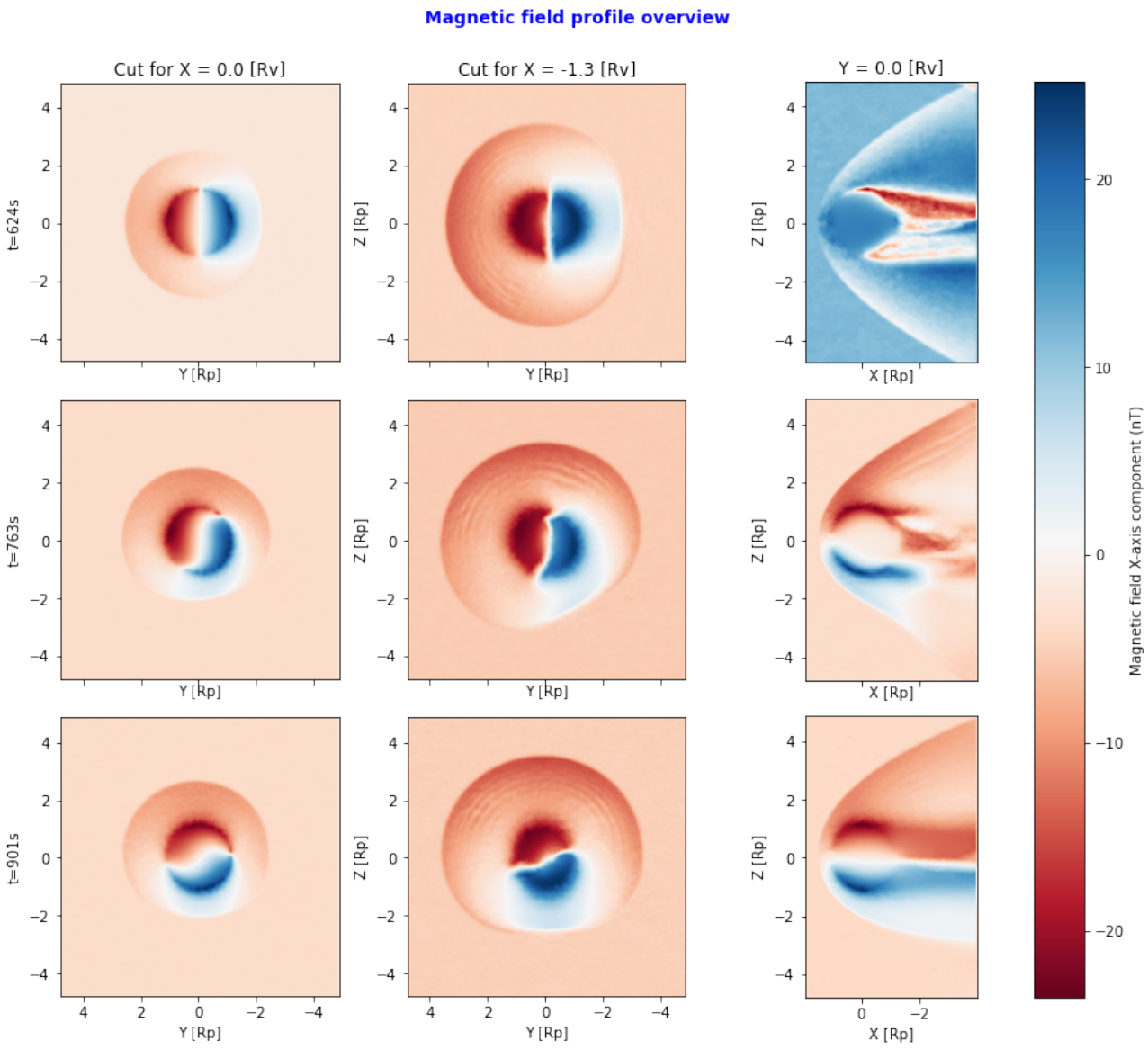

FIGURE 5 – Overview of the B_x component of the magnetic field in different planes and during different snapshots in time starting from the beginning of the IMF rotation ($t = 624s$)

Annular areas As stated earlier, for each plane the Bow Shock (of radius r_{BS}) and the Magnetic Pile-up Boundary (r_{MPB}) are what divides the study, alongside a fictional barrier a third of the way in between ($r_{mid} = r_{MPB} + \frac{r_{BS} - r_{MPB}}{3}$), into the following areas :

- The IMF area for $r \geq r_{BS}$, outside of the influence of the planet and its induced magnetosphere.
- The Outer Magnetosheath area for $r_{mid} \leq r < r_{BS}$ where solar wind experiences a slight slowing down and deviation

— The Inner Magnetosheath area for $r_{MPB} \leq r < r_{mid}$ where solar wind experiences a greater slowing down and deviation
— The Inner MPB area for $r < r_{MPB}$ where planetary and pick-up ions play a greater role

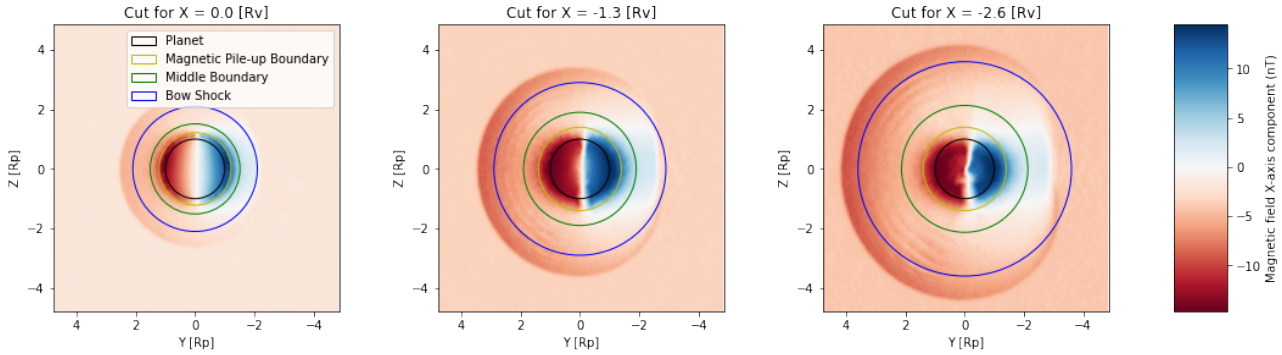

FIGURE 6 – Overview of the B_x component of the magnetic field in different planes and annular division of each plane

Here we followed the method by Romanelli et al. (2019)[10], but had to adapt it to the Venusian environment. Moreover, different definitions for the annular areas used here.
A big emphasis was placed on having areas that are consistent in some way from one plane to another is what led to this modification of the area division. In particular, the annular areas are defined in such a way that the flow of plasma ions through one area is always within the same area when propogated in space.
This guarantees that particles in one plane do not change areas after propagating downstream and end up in the same area in the following planes.

3.4 Clock angle derivation

Having defined clearly the different areas of interest and study, what is left is a consistent definition of a proxy to showcase the evolution and orientation of the induced magnetosphere. This proxy is what is called the clock angle and it is based on the draping shape around the planet that is shown in the following.

3.4.1 • Magnetic field draping

As the frozen-in magnetic field lines are carried by the solar wind, a very particular shape emerges from the slowing down of these plasma ions as they approach the planet and cross different boundaries. This has been a very well known and studied phenomenon dating as far back as a study by Saunders and Russell 1986[8]

This draping shape is characterized by an antisymmetry in the X component of the magnetic field between the magnetic dusk and dawn due to the stretching of the magnetic field lines

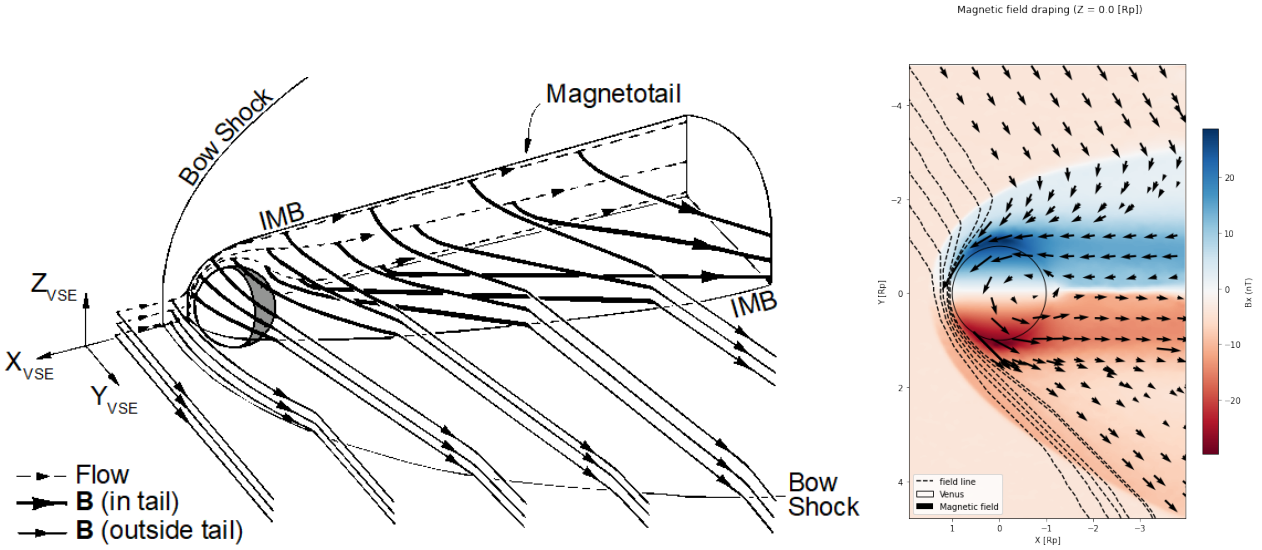

FIGURE 7 – Draping pattern around Venus : a typical example of the induced magnetosphere of an unmagnetized atmospheric object

further away from the planet.
The high directionality of this draping towards the direction of the IMF magnetic field makes for a good measure of the "orientation" of the magnetic field in a certain area and therefore can be used as a good proxy for this direction and allows us to compare it to the IMF direction at each point in time to recover what we dubbed the clock angle.

3.4.2 • CLOCK ANGLE DEFINITION

We consider three planes separated by $1.3R_V$. For each of these planes, we consider four annular regions delimited by the radial intervals whose edges we previously defined.
In each of these areas, we compute a unitary vector $\overrightarrow{\mathbf{r}}$ that will be a proxy to characterize the orientation of the corresponding region as follows :

- Divide the area in two lobes according to the the sign of B_x (B component along the Venus-Sun direction)
- Determine $\langle\overrightarrow{\mathbf{r}_+}\rangle$ and $\langle\overrightarrow{\mathbf{r}_-}\rangle$, the centers of respectively $B_x > 0$ and $B_x < 0$ lobe areas calculated as "centers of mass" for their respective lobes weighted with the magnetic field intensity in the x direction B_x :

$$\langle\overrightarrow{\mathbf{r}_+}\rangle = \frac{\sum B_x \times \overrightarrow{\mathbf{r}}}{\sum B_x} \text{ where } B_x > 0$$

$$\langle\overrightarrow{\mathbf{r}_-}\rangle = \frac{\sum B_x \times \overrightarrow{\mathbf{r}}}{\sum B_x} \text{ where } B_x < 0$$

- $\overrightarrow{\mathbf{r}}$ is the unitary direction vector from $\langle\overrightarrow{\mathbf{r}_+}\rangle$ to $\langle\overrightarrow{\mathbf{r}_-}\rangle$

In absence of rotation, during equilibrium, all the areas are aligned with the IMF direction is as the magnetic field draping occurs around Venus.

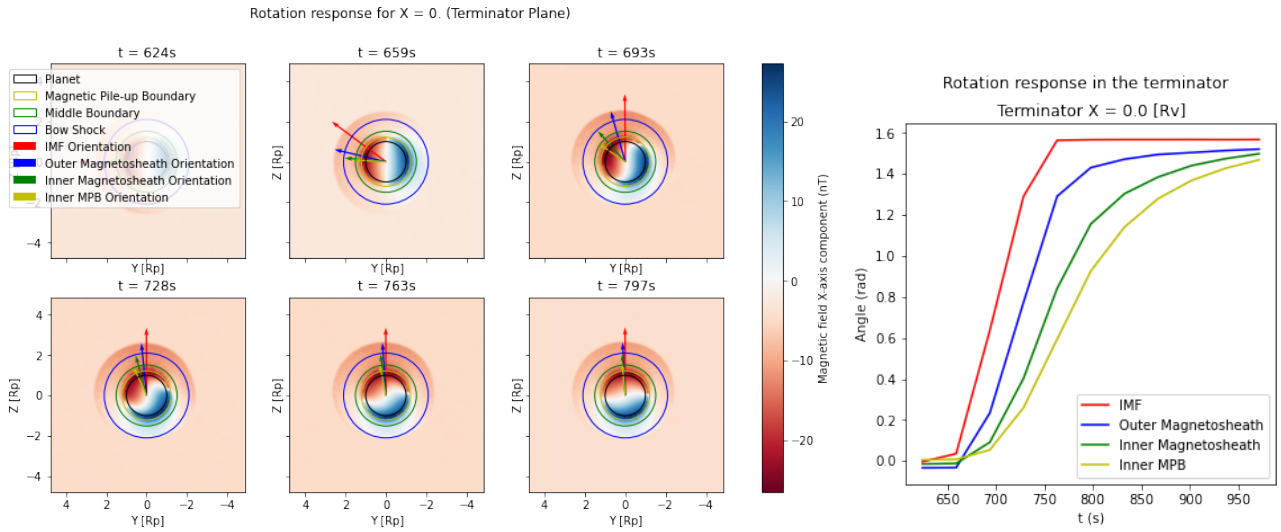

FIGURE 8 – Rotation response in the terminator and angle evolution for each annular area

Figure 8 is an overview of the method applied in the case of the terminator plane.
The right plot shows the calculated angles and the evolution of each area's orientation as a function of time. The clock angle for a certain area at a time t would be the difference between the current angle for the area and the IMF (red curve).
As for the left plot, an overview of B_x the X component of the magnetic field in the terminator is plotten through different snapshots in time. Boundaries are also superposed on these plots and colored arrows pointing in the calculated directions of the corresponding area are drawn with (0,0) as an origin.
The figure showcases how different areas respond differently and how they adapt and catch up to the IMF rotation.

This method uses this draping alignment to gauge the clock angle deviation of each area from the IMF orientation in the same plane.

4 ANALYSIS AND RESULTS

We begin our analysis of the results from our different simuation runs by checking the general profiles of the rotation responses.
Using the previous methods, we consider the beforementioned YZ-VSO plane cuts at X-VSO respectively equal to $0.0R_V$, $-1.3R_V$ and $-2.6R_V$.

The Bow Shock, modelled as a conic curve defined by the equation $r = \frac{L}{1+\epsilon\cos(\theta)}$ in cylindrical coordinates, intersects each of these planes in a circle. With the fitted values for :

- The eccentricity of the conic curve $\epsilon = 1.028 \pm 0.010$
- The focus point $x_0 = (0.691 \pm 0.032)R_V$
- The semilatus rectum $L = (1.499 \pm 0.041)R_V$

We find the intersection circles to be respectively, each centered around $(Y, Z) = (0, 0)$ in their respective planes :

- In the terminator plane : $R_{terminator} = 2.1R_V$
- In the middle plane for $X = -1.3R_V$: $R_{midway} = 2.9R_V$
- Downstream in the $X = -2.6R_V$ plane : $R_{down} = 3.6R_V$

As for the Magnetic Pile-up Boundary, we derive its radius in each plane as the radius of pressure equality $P_{th} = P_{mag}$ between the plasma thermal pressure and the magnetic pressure.

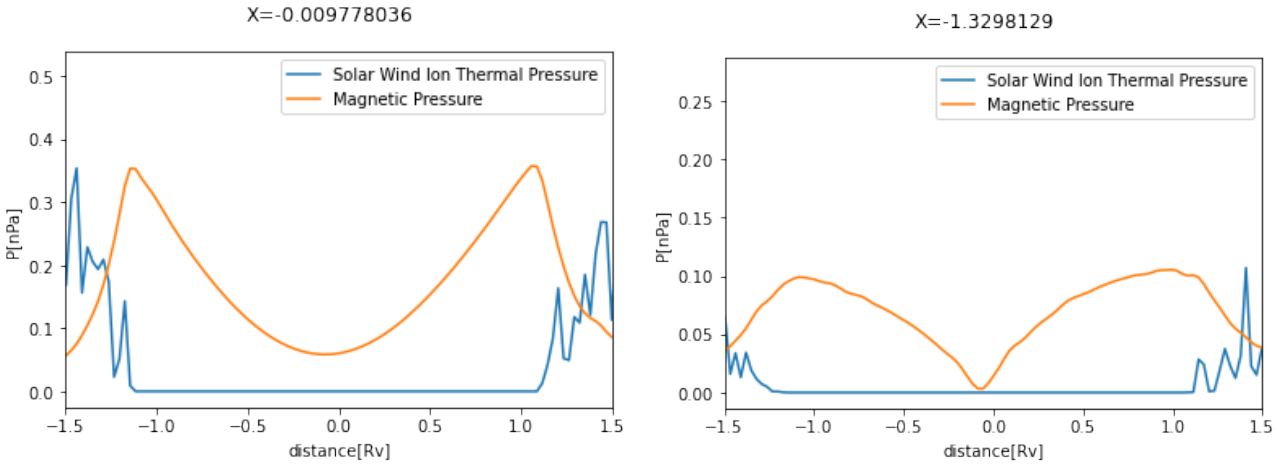

FIGURE 9 – Pressure profiles

The derived values are as follows in our test simulation run :

- In the terminator plane : $r_{terminator} = 1.22R_V$

— In the middle plane for $X = -1.3R_V$: $r_{midway} = 1.4R_V$
— Downstream in the $X = -2.6R_V$ plane : $r_{down} = 1.4R_V$

Boundary Radii	In the Terminator (X=0.0 Rv)	At X=-1.3 Rv	At X= -2.6 Rv
Bow Shock	2.1 Rv	2.9 Rv	3.6 Rv
Middle Boundary	1.51 Rv	1.9 Rv	2.13 Rv
Magnetic Pile-up Boundary	1.22 Rv	1.4 Rv	1.4 Rv

FIGURE 10 – Radii used for boundaries to define the annular regions in our analysis

4.1 RECOVERY PROFILE

This section aims to showcase the recovery-timescales for each areas in an effort to understand the time delays experienced in the adaptation of the clock angle to the IMF rotation.
We aim to explain these delays and link them to plasma physical properties, namely the plasma velocity and its consequences on the delay linked to the solar wind propagantion from an area to the next.
The slowing down of the plasma in the near-planetary area would contribute to this delay, its dependence in space and its variations between different areas considered.

For this analysis, we compare results from three different IMF rotation routines, each with different angle rotation speeds, all starting at the same time $t = 626.580s$ in the simulation.
The first test run is one where the IMF rotates by 90° from its initial orientation in a time frame of $83.544s$.
The other runs, twice as fast and twice as slow respectively, rotate by the same angle during $41.772s$ and $167.088s$.

Figure 5 shows the calculated angle evolution in time in different areas at different distances in space.

The IMF orientation is derived from sampling the orientation of the magnetic field projected vector in each plane, while for other areas the previously defined method using the division into positive and negative B_x components and finding the direction connecting both areas is used.

As predicted, the IMF rotation propagates both downstream and inwards with different time delays. For instance, when comparing similar annular regions, the clock angle varies first in the plane that is furthest upstream as the magnetic perturbation propagates through the system.

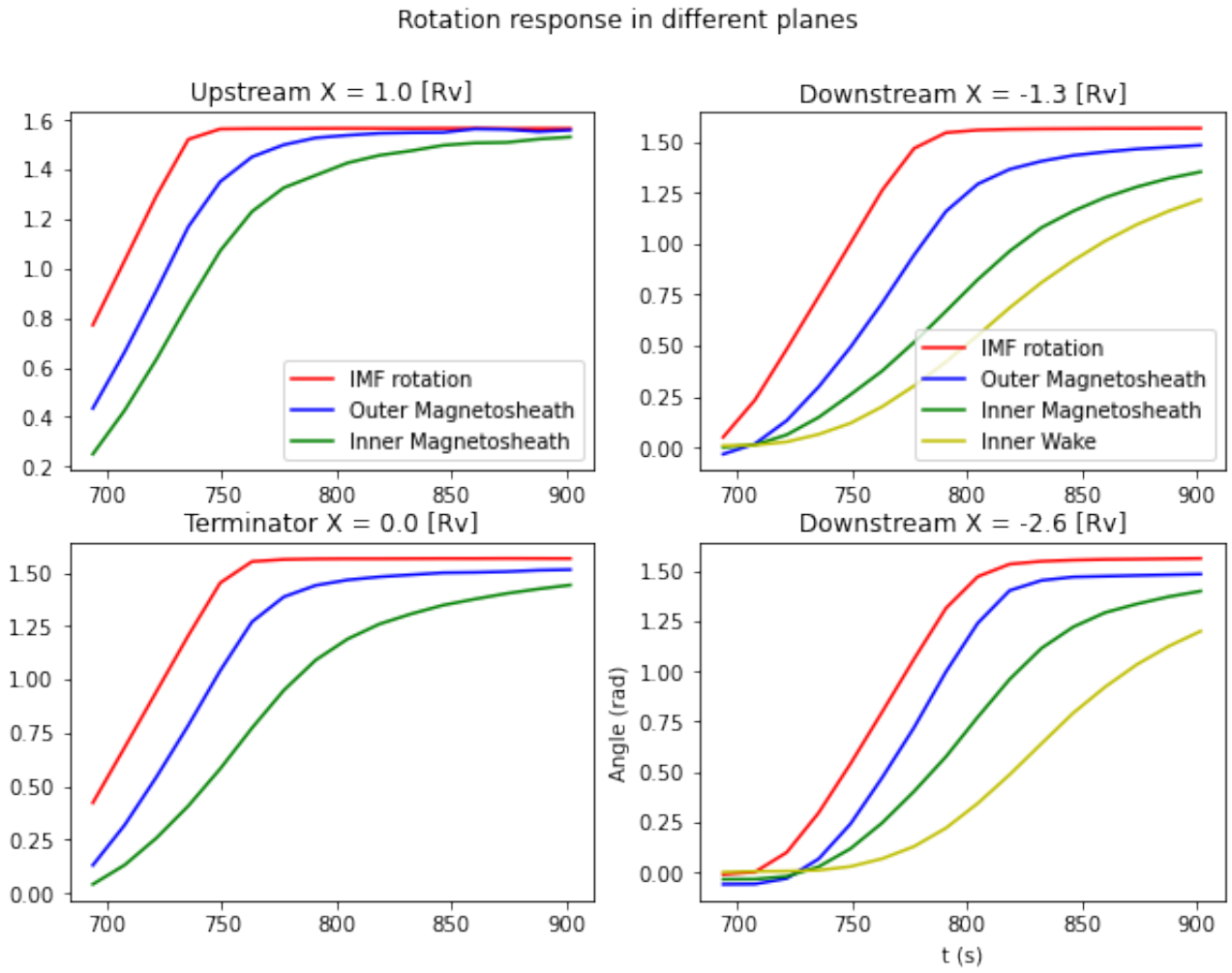

FIGURE 11 – Recovery profiles at multiple areas of the Venusian environment

We therefore observe a linear time delay from one plane to the next that we endeavor to prove is linked to the propagation times of the Solar Wind ions that carry the "frozen-in" magnetic field lines.
Comparing annular regions in the same plane shows not only a larger time shift but also a smoother rotation of the local magnetic field for the innermost areas.

The rotation velocity drop for the inner or closer to the planet regions suggests the effect of resistive and inductive phenomenon in delaying the adaptation of the local magnetic field to the IMF rotation. We focus our study of these clock angle rotation velocities in the following section.

4.2 Clock Angle rotation velocities

As stated earlier, inner regions experience slower rotations and smoother adaptations to the IMF perturbations.
We endeavor to describe the global response of each area in terms of adaptation speed. We therefore assign non time-dependent velocity values to each area as follows.

The velocities of each areas are calculated from the angle evolution curves as the maximum slopes, or slopes in the inflexion point of the curve.
The evolution of these velocities between the terminator and the downstream planes is of interest here, and seems to follow an interesting evolution as seen from the analysis of the test run.

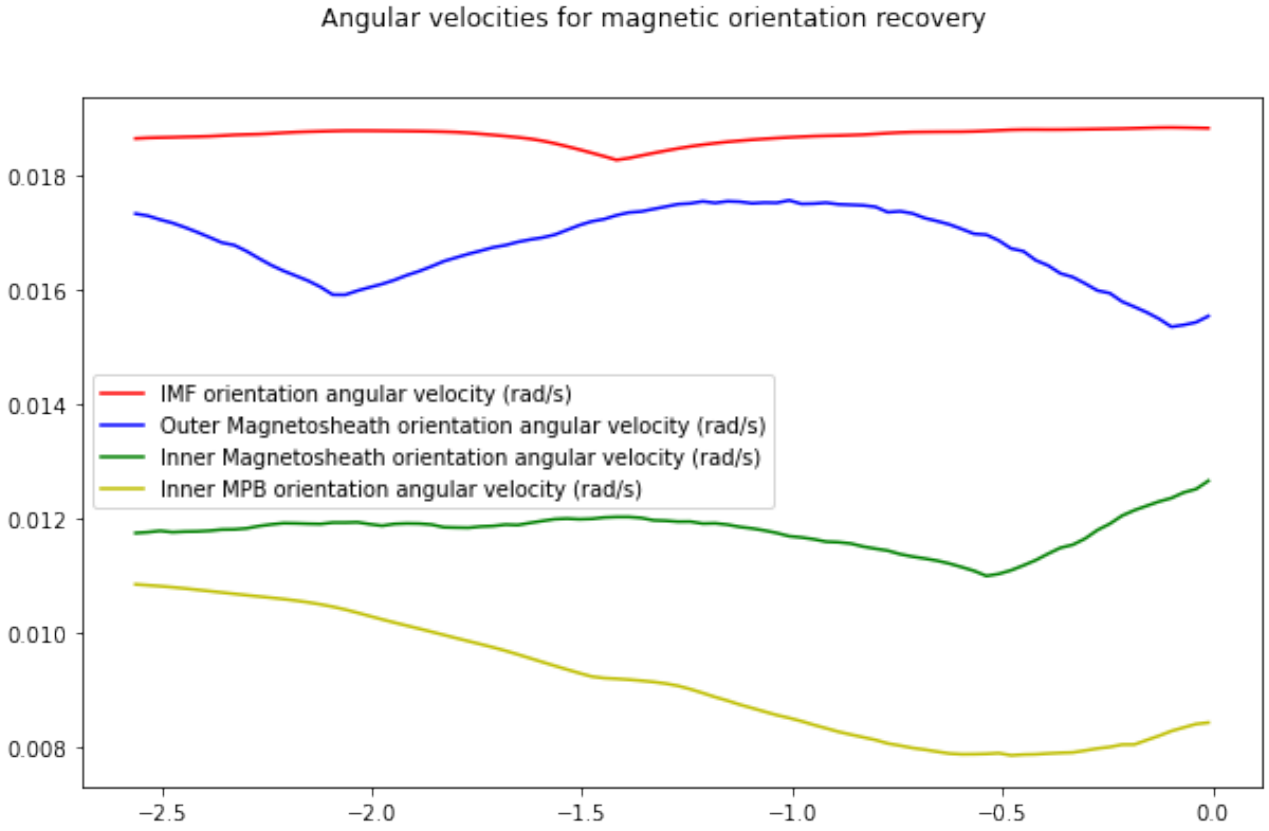

Figure 12 – Rotation velocities $[rad.s^{-1}]$ per area according to X-coordinate $[R_V]$

We can see on this figure that regardless of the X coordinate, the rotation velocity is all the slower as we consider more inward areas that are closer to the planet's vicinity. We can see from this example how these areas experiece a dip in velocity near the planet, presumabily due to interactions with the Venusian environment, and that the outermost area is relatively fast compared to more inner areas that experience a dip in velocity compared to the rotation of the

IMF in the corresponding plane.

Comparisons can also be made in the slower and faster rotation cases, the results are widely different as shown in the plots that follow.
Compared to our test case, the most significant changes happen for the outermost areas.

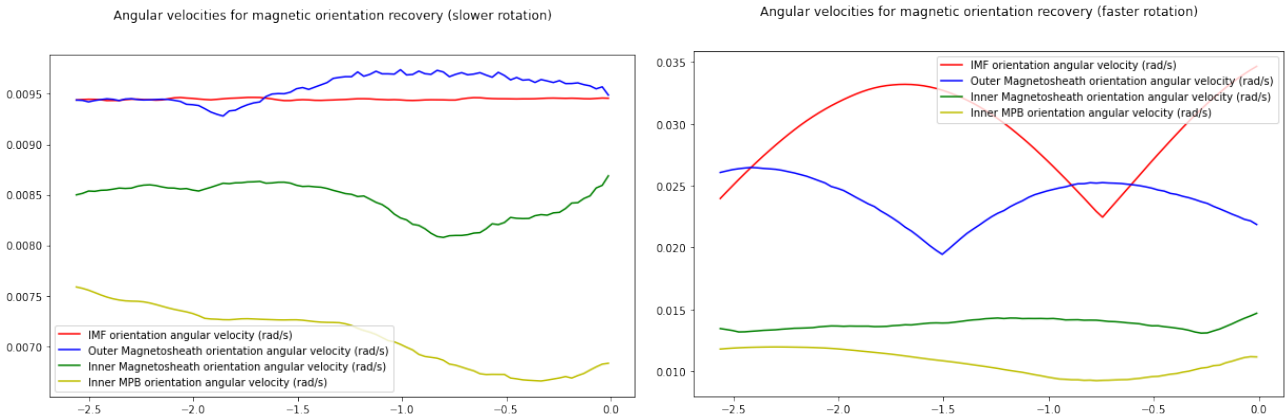

FIGURE 13 – Rotation velocities $[rad.s^{-1}]$ per area according to X-coordinate $[R_V]$

The inner Magnetosheath and MPB areas seem to behave in a similar way, rotating relatively faster when the IMF rotation is more gradual and slower when the IMF rotation happens more suddenly.

For the slower rotation case, the outer magnetosheath keeps up more easily with the perturbation which leads to adaptive rotation that closely matches the IMF rotation in speed.

When the IMF rotates faster however, the results are more hectic and unpredictible. The IMF rotation in each plane seems to vary more greatly between planes and so does the outer magnetosheath area. In some planes the IMF area is slower than the outer magnetosheath, and in others it greatly surpasses it in rotation velocity.
Moreover, it is almost as if the outer magnetosheath area follows the velocity curve of the IMF area with a "spacial delay" in the X-axis.

4.3 Link to solar wind movement

We show that linear time delays for the IMF rotation can be linked to the duration for the propagation of the solar wind particles downstream.
These particles are slowed and deviated as they breach the BS and approach the venusian environment. The more "central" (closer to the planet) particles are more affected by this deviation, which would explain the greater slowing down of the rotation in more inner areas. Specifically,

the particles carry the frozen-in magnetic field lines. The propagation of perturbations in the IMF are also carried by these same particles.
We then expect the timescales for the IMF rotation to propagate in the X-axis, direction of the flow of the solar wind plasma particles, to correspond to the propagation time of these particles in the X-direction. This is what we try to confirm numerically in the next section.

4.3.1 • Solar wind movement

In our simulations, the solar wind is constantly flowing as a plasma in the X-direction, with the upstream conditions determining its state and its interaction with the Venusian environment. This is for instance why the rotation in the simulation doesn't start right away, but rather runs with the initial conditions for a while so as to reach an equilibrium state before starting the perturbations.

The flow of the solar wind is the mecanism suspected to carry the propagation of IMF rotation and hence the recovery of the induced magnetosphere. Specifically, its variation as the plasma interacts with Venus and affects the flow direction and velocities, is a big part of the observed delays and disparities in the timescales for clock angle variabilty.
The in-depth study of the spacial evolution and flow of the plasma particles in multiple space and time coordinates, allowed thanks to the powerful tool that is the hybrid simulations, helps us gain a better understanding and highlight the link between particle flow and the magnetospheric response to the IMF rotation. For instance, the hybrid simulation can be used to determine the movement of particles as they propagate from a plane to another (in the X direction). We can verify this way that the areas considered in each plane are not arbitrary, but connected to each other through the flow of the solar wind between them.

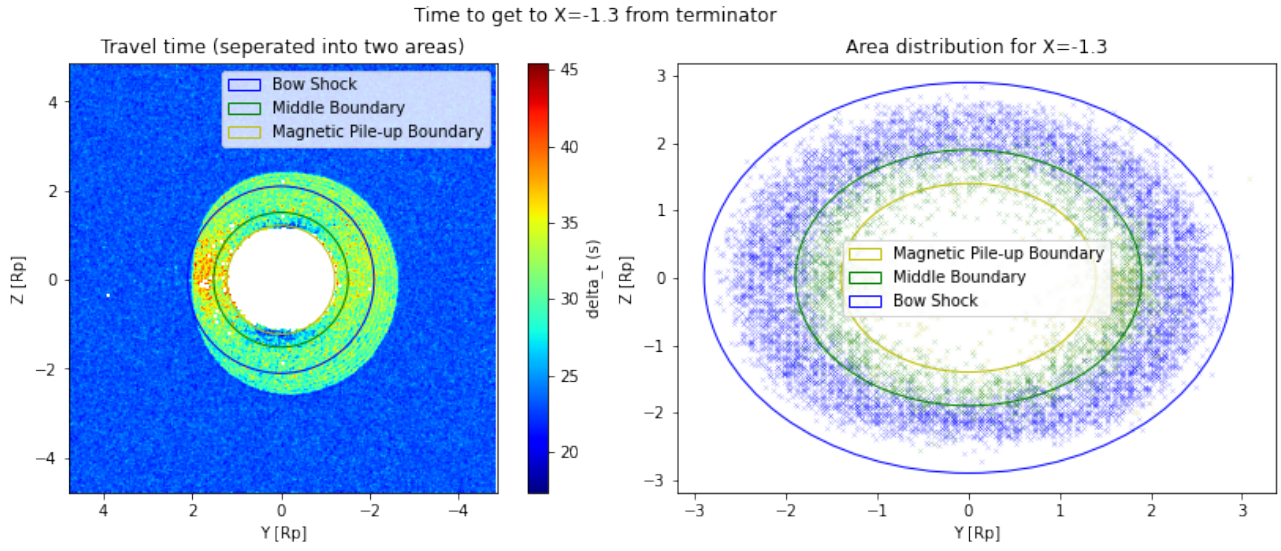

Figure 14 – Study of the propagation of the solar wind from the Terminator downstream

Figure 14 shows how the solar wind moves both radially and in the X direction as it travels from the terminator to $X = -1.3R_V$. Boundaries relative to each plane are traced in both corresponding figures.
The left figure is a colormap of the average time for each gridpoint, or for the particles populationg said gridpoint, to reach the goal plane at $X = -1.3R_V$. This time is, as shown by the figure, different in each area as the inner areas experience more significant slowing down in the considered direction.
The right figure is also a cut but for the plane at $X = -1.3R_V$, it is a showcase of where particles flowing from the terminator end up radially as they reach this plane.
The right figure shows consistency between area definitions in each planes, as the particles within the green boundary (color coded in green) in the terminator arrive within the green boundary in the following plane. Particles between this boundary and the blue one (color coded in blue) in the terminator also arrive within the boundary and out of the green one in the following plane.

The flow of the particles is determined in the simulation from the movement of what we called "macroparticles".
In fact, the simulation being divided in a grid structure, each grid block has its average characteristics like particle density, velocity and pressure calculated at each time step.
The average movement of particles within a grid block is therefore accessible through these values and they can be used to describe the flow of plasma on a larger scale.

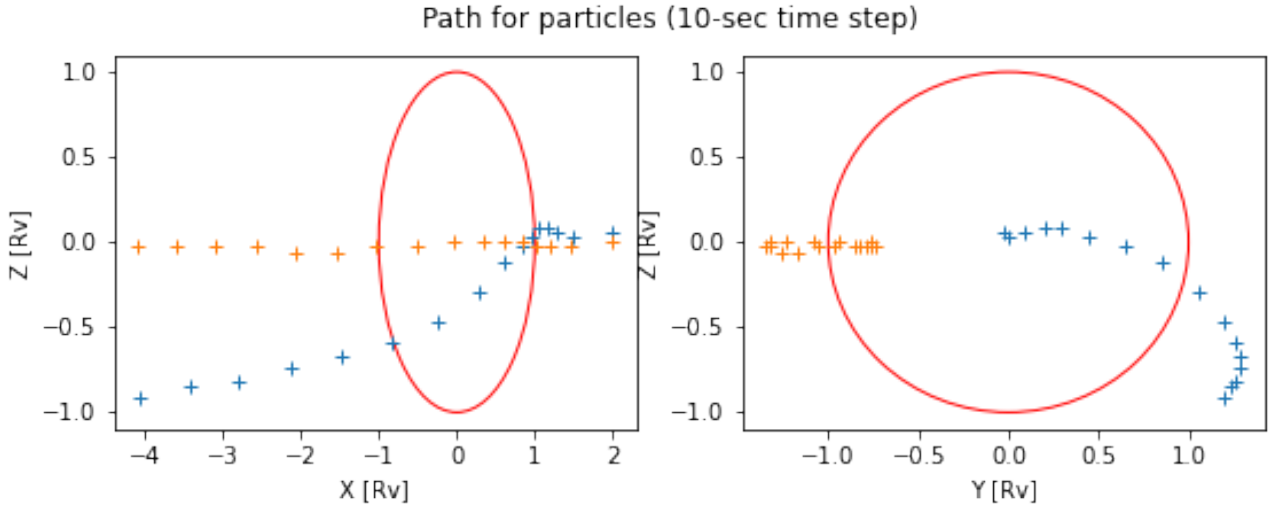

FIGURE 15 – Particle movement viewed from different perspectives

For example, in Figure 15, the movement of the "macroparticles" that travel between grid blocks is traced and snapshots are taken around every 10 seconds.
Two examples are plotted in this figure, starting at the same time with the same X coordinate at $+2R_V$.

The left figure shows how particles are slowed down (closer distance between snapshots) and deviated as they approach the planetary environment. They are then accelerated again when they have moved past the planet.
The right figure shows in more detail how they are deviated and end up farther from the center as they travel downstream.
The orange path is interestingly relatively stable when it comes to its Z coordinate, whereas the blue path is more typical and although starting very close to the center, contours the planet and ends up a fair distance away radially.

Although an accurate analysis can be followed for each path for solar wind flow by minimizing time-steps and having accurate paths with time dependent velocities, for most cases tried in this study where the solar wind is travelling downstream, a first order approximation has been suffecient.
For determining the time needed for particles to travel from plane-to-plane and their radial positions in the target plane can be approached by a linear propagation from the starting plane, knowing the velocities in each direction at the starting time.

4.3.2 • Link to magnetospheric recovery

With the simulation allowing for an in depth analysis of time delays, both for the movement and flow of the solar wind plasma particles and for the adaptability of the Venusian induced magnetosphere.

The hypothesis that the perturbations in the IMF angle are carried by the solar wind movement impies that the time delays for clock angle rotation would follow the travel times of the solar wind.
This can be verified within the simulations in a area-to-area comparison, by propagating an area's recovery profile to the same area in the following plane.
This is where the verification of correspondance of areas in different planes comes into play and is important for the comparisons to be legitimate and to make sense.

Comparisons are made and visualized in Figure 16 ; each area from the starting plane is assigned its average time for particles to reach the following plane starting from their position. It can be approximated from knowing the average velocity U_X in the X direction.
The recovery and angle evolution profiles are also calculated for the corresponding plane, giving different curves for each areas.
The expected profiles in the following plane are then determined from these calculations : each area has its curve delayed by a linear time that is the particle travel time to the next plane.
This would fit the "observed" recovery curve in the target plane in the simple case where perturbations are carried by the movement of the particles in the solar wind plasma.

These expected curves, shown here with dotted lines, are drawn to compare profile propagated from the terminator to the calculated profiles in the following planes.

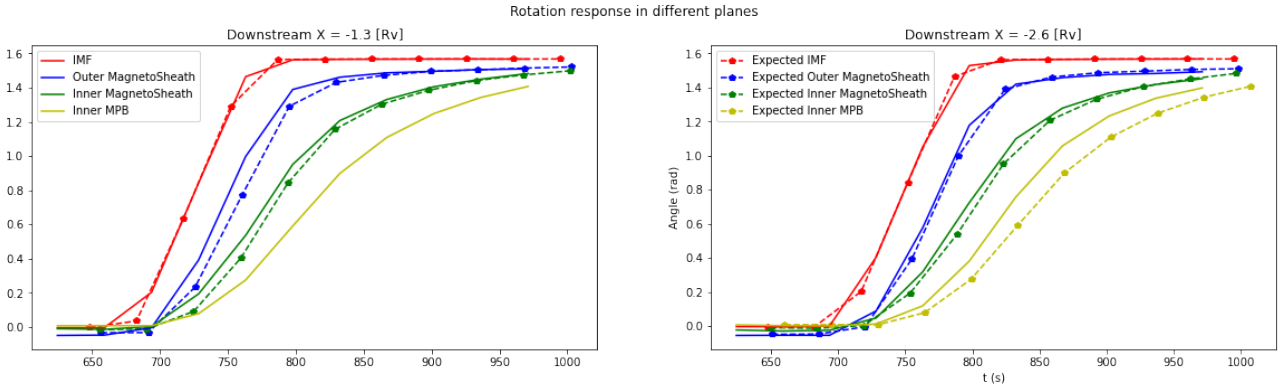

FIGURE 16 – Comparison between rotation profiles for the same areas between different planes

What analysis shows is that for the areas outside of the MPB, these curves match closely and are within the error bars ; In fact, if we take into account the average rotation of the particles between planes, which would drag the magnetic field lines and therefore the calculated orientation angles in this model, it is found to be within the same order of magnitude of the distances between actual and expected curves.
For instance, ions rotate by angles of the order of 0.05 *rad* while flowing from the terminator to the $X = -1.3R_V$ plane or from the latter plane to $X = -2.6R_V$.

This model proves, as seen in the right plot, less accurate for the inner MPB area (yellow curves) or the wake downstream of the planet.
We can see that in the right plot that other than the linear time delay, the expected angle is slower in rotation compared to the actual one as the slopes of the yellow curves do not match. The effects of planetary "pickup ions", as well as other phenomenon like magnetic reconnection that might accelerate or descelerate the rotation of the clock angle.
A detailed analysis of these effects is out of scope for this study, and is a potential direction for further analysis

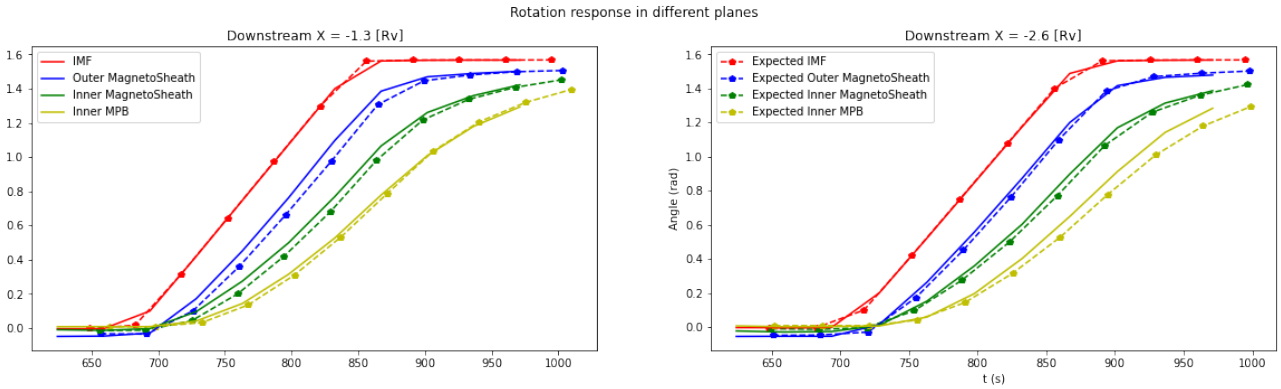

FIGURE 17 – Comparison between rotation profiles : cases for slower IMF rotation

The same study has also been extended to the slower and faster rotations of the IMF to confirm the results observed.

Here again, the expected curves match the calculated ones very closely and within range of the error bars, with only the exception of the downstream Inner MPB area.
Otherwise, the distances shown are within the error bars and can be explained by ion rotation around the X axis.

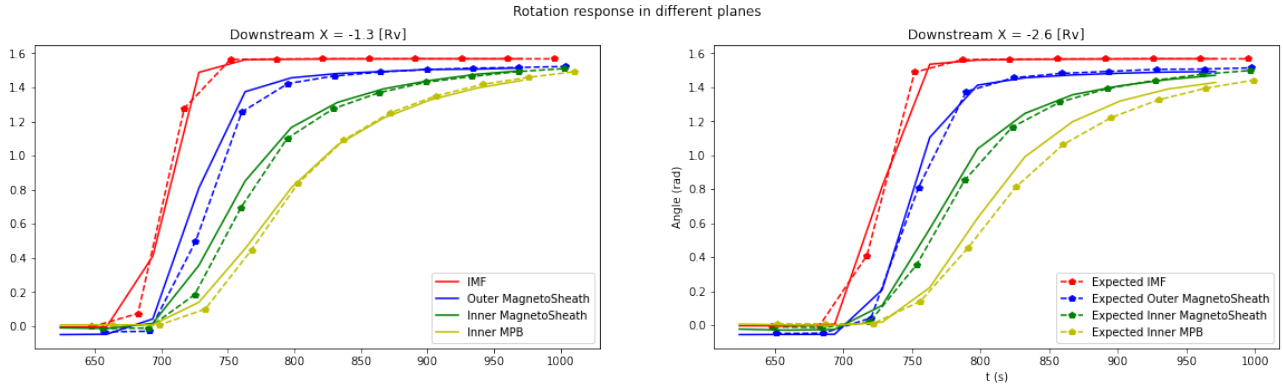

FIGURE 18 – Comparison between rotation profiles : cases for faster IMF rotation

5
DISCUSSION AND CONCLUSIONS

This work aims to explore and advance the study of unmagnetized celestial objects and specifically how they interact with the plasma and magnetic field environment of the heliosphere.

It shows how the Venusian induced magnetosphere formed in response to the overlying magnetic field known as the IMF (Interplanetary Magnetic field) responds to variations and perturbations in this magnetic field. In particular, it shows how closely related this adaptive response to perturbations in the IMF is to the propagation of solar wind ions in the Venusian environment, suggesting that this recovery is mainly carried through physical phenomenon such as the movement of particles traversing the planet's vicinity.

This study shows that in the case of a rotation of the IMF upstream of the planet with non significant change to its amplitude nor to the solar wind characteristics (density, velocity, ...), the rotation is replicated in the Venusian induced magnetosphere that realigns with the IMF with time delays that depend on the area considered. Linear time delays increase further downstream and more central or closer to the planet zones experience an additional delay in their reaction.

The linear time delays can be compared to the travel times linked to the solar wind flow and velocity. The simulation results downstream of the planet show correspondance between the times for solar wind to travel from an area to the next and the time delay in the rotation response between these areas. This correspondance holds regardless of which area we consider between the Venusian Bow Shock region and the Ion Composition Boundary, within which other phenomenon affect and may slow down the adaptability of the magnetosphere to IMF perturbations.
The plasma having experienced different levels of slowing depending on the area's distance from the planet, the previous result is in alignment with the hypothesis where the perturbations are carried and propagated by the solar wind plasma particles flowing downstream.

An interesting follow up to this study, which also tackles how the timeframe within which such IMF perturbation happens affects the adaptive response of the magnetosphere, is to expand to how different variables such as the solar wind parameters would affect such results.

It would also be interesting to explore the phenomenon happening closer to the planet or in its wake and their effect on the adaptability of these regions to the IMF rotations.

RÉFÉRENCES

[1] Solar wind interaction and impact on the venus atmosphere | space science reviews.

[2] S. Aizawa, M. Persson, T. Menez, N. André, R. Modolo, V. Génot, B. Sanchez-Cano, M. Volwerk, J. Y. Chaufray, C. Baskevitch, D. Heyner, Y. Saito, Y. Harada, F. Leblanc, A. Barthe, E. Penou, A. Fedorov, J. A. Sauvaud, S. Yokota, U. Auster, I. Richter, J. Mieth, T. S. Horbury, P. Louarn, C. J. Owen, and G. Murakami. LatHyS global hybrid simulation of the BepiColombo second venus flyby. 218 :105499.

[3] Lihui Chai, Markus Fraenz, Weixing Wan, Zhaojin Rong, Tielong Zhang, Yong Wei, Eduard Dubinin, Jun Zhong, Xiuhong Han, and Stas Barabash. IMF control of the location of Venusian bow shock : The effect of the magnitude of IMF component tangential to the bow shock surface. *Journal of Geophysical Research : Space Physics*, 119(12) :9464–9475, 2014. _eprint : https ://onlinelibrary.wiley.com/doi/pdf/10.1002/2014JA019878.

[4] Yoshifumi Futaana, Gabriella Stenberg Wieser, Stas Barabash, and Janet G. Luhmann. Solar wind interaction and impact on the venus atmosphere. 212(3) :1453–1509.

[5] M. K. G. Holmberg, N. André, P. Garnier, R. Modolo, L. Andersson, J. Halekas, C. Mazelle, M. Steckiewicz, V. Génot, A. Fedorov, S. Barabash, and D. L. Mitchell. MAVEN and MEX Multi-instrument Study of the Dayside of the Martian Induced Magnetospheric Structure Revealed by Pressure Analyses. *Journal of Geophysical Research : Space Physics*, 124(11) :8564–8589, 2019. _eprint : https ://onlinelibrary.wiley.com/doi/pdf/10.1029/2019JA026954.

[6] C. Martinecz, M. Fränz, J. Woch, N. Krupp, E. Roussos, E. Dubinin, U. Motschmann, S. Barabash, R. Lundin, M. Holmström, H. Andersson, M. Yamauchi, A. Grigoriev, Y. Futaana, K. Brinkfeldt, H. Gunell, R. A. Frahm, J. D. Winningham, J. R. Sharber, J. Scherrer, A. J. Coates, D. R. Linder, D. O. Kataria, E. Kallio, T. Sales, W. Schmidt, P. Riihela, H. E. J. Koskinen, J. U. Kozyra, J. Luhmann, C. T. Russell, E. C. Roelof, P. Brandt, C. C. Curtis, K. C. Hsieh, B. R. Sandel, M. Grande, J. A. Sauvaud, A. Fedorov, J. J. Thocaven, C. Mazelle, S. McKenna-Lawler, S. Orsini, R. Cerulli-Irelli, M. Maggi, A. Mura, A. Milillo, P. Wurz, A. Galli, P. Bochsler, K. Asamura, K. Szego, W. Baumjohann, T. L. Zhang, and H. Lammer. Location of the bow shock and ion composition boundaries at venus—initial determinations from venus express ASPERA-4. 56(6) :780–784.

[7] Ronan Modolo, Sebastien Hess, Marco Mancini, Francois Leblanc, Jean-Yves Chaufray, David Brain, Ludivine Leclercq, Rosa Esteban-Hernández, Gerard Chanteur, Philippe Weill, Francisco González-Galindo, Francois Forget, Manabu Yagi, and Christian Mazelle. Mars-solar wind interaction : LatHyS, an improved parallel 3-d multispecies hybrid model. 121(7) :6378–6399. _eprint : https ://onlinelibrary.wiley.com/doi/pdf/10.1002/2015JA022324.

[8] J. L. Phillips, J. G. Luhmann, and C. T. Russell. Magnetic configuration of the venus magnetosheath. 91 :7931–7938. _eprint : https ://onlinelibrary.wiley.com/doi/pdf/10.1029/JA091iA07p07931.

[9] John L. Phillips and David J. McComas. The magnetosheath and magnetotail of venus. 55(1) :1–80.

[10] N. Romanelli, G. DiBraccio, R. Modolo, F. Leblanc, J. Espley, J. Gruesbeck, J. Halekas, J. Mcfadden, and B. Jakosky. Recovery timescales of the dayside martian magnetosphere to IMF variability. 46(20) :10977–10986.

[11] C. Signoles, M. Persson, Y. Futaana, S. Aizawa, N. André, S. Bergman, A. Fedorov, V. Lindwall, N. Martinez, C. Mazelle, S. Rojas Mata, A. Wolff, and T. L. Zhang. Influence of solar wind variations on the shapes of venus' plasma boundaries based on venus express observations. 954(1) :95. Publisher : The American Astronomical Society.